Journal of Power Sources 256 (2014) 96–101

Contents lists available at ScienceDirect

Journal of Power Sources

journal homepage: www.elsevier.com/locate/jpowsour

Performance evaluation of a non-woven lithium ion battery separator prepared through a paper-making process

Xiaosong Huang*

Chemical & Materials Systems Lab, GM Global R&D, 30500 Mound Rd, Warren, MI 48090, USA

HIGHLIGHTS

- Composite separators have been successfully developed using a paper-making process.
- The composite separators show good thermal stability and electrolyte wettability.
- Cells with the composite separators exhibit good cycling performance.
- The composite separators also enabled excellent cell rate capability.

ARTICLE INFO

Article history:
Received 15 November 2013
Received in revised form
6 January 2014
Accepted 17 January 2014
Available online 24 January 2014

Keywords:
Composite separator
Non-woven
Thermal performance
High rate capability
Lithium ion battery

ABSTRACT

Porous separator functions to electrically insulate the negative and positive electrodes yet communicate lithium ions between the two electrodes when infiltrated with a liquid electrolyte. The separator must fulfill numerous requirements (e.g. permeability, wettability, and thermal stability) in order to optimize the abuse tolerance and electrochemical performance of a battery. Non-woven mat separators have advantages such as high porosity and heat resistance. However, their applications in lithium ion batteries are very limited as their inadequate pore structures could cause accelerated battery performance degradation and even internal short. This work features the development of thermally stable non-woven composite separators using a low cost paper-making process. The composite separators offer significantly improved thermal dimensional stability and exhibit superior wettability by the liquid electrolyte compared to a conventional polypropylene separator. The open porous structures of the non-woven composite separators also resulted in high effective ionic conductivities. The electrochemical performance of the composite separators was tested in coin cells. Stable cycle performances and improved rate capabilities have been observed for the coin cells with these composite separators.

1. Introduction

Secondary lithium ion batteries appeal to many users because they offer a high specific energy, a high energy density, a long cycle lifetime, a low self-discharge rate, and a high operational voltage [1]. Their four major components are the positive electrode, the negative electrode, the electrolyte, and the separator that is disposed between the two electrodes. The porous separator functions to physically and electrically insulate the negative and positive electrodes yet communicate lithium ions between them when infiltrated with the liquid electrolyte. The separator property is one of the key factors that directly affect the abuse tolerance and electrochemical performance of a battery.

Porous polyolefin membranes are the most widely used lithium ion battery separators due to their good electrochemical and chemical stability, very low moisture absorption, and excellent tensile properties. However, the processes of making conventional separators require precise stretching of the extruded thin film to create pores [2–4]. Heat exposure to these stretched separators initiates re-coiling of the elongated polymer chains, observed as membrane shrinkage, which could significantly increase the risk of battery shorting, especially for large format battery applications. In addition, the melting temperature of polyolefin is normally in the range of 120–170 °C. Any local hot spots developed under abnormal conditions could cause the melting of the separator further increasing the contact area between the two electrodes.

Non-woven mat separators have been widely used in several types of batteries because they normally have high porosity, good chemical resistance, and excellent thermal stability. However, the major barriers to using non-woven separators in lithium ion

* Tel.: +1 586 9860836; fax: +1 586 9861207.
E-mail address: xiaosong.huang@gm.com.

0378-7753/$ – see front matter © 2014 Published by Elsevier B.V.
http://dx.doi.org/10.1016/j.jpowsour.2014.01.080

batteries have been their large pore size and the difficulty in making thin (<25 μm) uniform non-wovens. In recent years, non-woven separators made of novel sub-micron sized fibers have been developed and tested in lithium ion batteries [5–12]. Non-woven mats of polyacrylonitrile (PAN), polyvinylidene fluoride (PVDF), and polymer blends of polyimide with porosities ranging from 65 to 85% have been prepared with a relatively slow electro-spinning process [5–7]. Those electrospun separators have shown negligible shrinkages at elevated temperatures and enabled good ionic conductivities. However, these polymers can be plasticized by liquid electrolytes leading to reduced mechanical properties. Wet-laid or air-laid non-woven fabrics based on thermalplastic polymers have also been evaluated as lithium ion battery separators [8–12]. They exhibited good dimensional stability at elevated temperatures as well as high effective ionic conductivities.

This report discusses the development and performance characterization of cellulose nanofiber based composite separators. A wet-laid process was bench-scaled to prepare the composite separators comprising cellulose fibers and ceramic particles. Cellulose is the most abundant biorenewable material, and natural cellulose fibers have excellent mechanical strength and thermal stability. The ceramic particles have been used to conveniently control the permeability of the composite separators. The other two potential functions of the ceramic particles include improving the non-woven mat uniformity and increasing the mat resistance to dendrite (or metal particle) penetration due to their excellent compressive strength.

2. Materials and experimental

The fiber used in this investigation was Celish micro-fibrillated cellulose (MFC) (Daicel Finechem Ltd) [13]. MFC is a micro-fibrillated cellulose made from highly refined pure plant fibers through a strong mechanical shearing force provided by a super-high-pressure homogenizer. It has a highly branched structure and the fiber diameter can be from 0.1 to 0.01 μm. The ceramic powder was a 1 μm alumina. Technical grade acetone was purchased from Sigma–Aldrich (St. Louis, MO). The anode and cathode materials used to make the full cells were TIMREX SLP 30 graphite and $LiNi_{1/3}Co_{1/3}Mn_{1/3}O_2$ (NCM) (Toda NCM-01ST-100), respectively. The electrolyte used was 1 M $LiPF_6$ in ethylene carbonate (EC)/dimethyl carbonate (DMC) 1:1 (v/v) (Novolyte Technologies).

The preparation of the MFC composite mats was achieved by a wet-laid (paper-making) process. The schematic is shown in Fig. 1. Controlled amounts of cellulose fibrils and alumina were weighed and mixed in distilled water by a bench scale shear blending for ~10 s. The uniform dispersions were filtered in a batch process onto two layers of 100 mesh screens and then dried in an oven at 80 °C for 2 h. Upon the careful removal from the mesh, composite mats with thicknesses of >35 μm were obtained. The final step of compressing the mats improved the mat uniformity and increased their mechanical properties. The mats were compressed under a pressure of 3 MPa for 20 s at room temperature between two parallel plates on a 50 Ton PHI hand press (SRPRSS-8004). The composite separators were then dried at 120 °C overnight before the characterization of their properties. In addition, the pressed mats were coated with porous polyvinylidene fluoride (PVDF) (Kynar® 761) by dipping in a coating bath consisting of a solution of 0.6 g of PVDF dissolved in a mixture of 0.4 g of distilled water and 14 g of acetone. A porous PVDF structure was formed with the evaporation of acetone via the well-known phase inversion process. The PVDF coating was added to augment the separator mechanical strength, keep ceramic particles from falling off, and improve the separator surface uniformity. The coated composite mats were then dried at 120 °C overnight for characterizations.

The surface morphologies of the composite mats were examined using a scanning electron microscopy (SEM). Samples were sputter coated with gold and exposed to an accelerating voltage of 5 kV.

The separator porosities were estimated using the equation below:

$$P = \frac{w_T - w_s}{\rho_l \cdot V_s}$$

where w_s is the weight of the dry separator sample, w_T is the weight of the separator once a liquid is fully absorbed, ρ_l is the density of the liquid, and V_s is the apparent volume of the sample.

The air permeability of the free-standing mats was tested on a capillary flow porometer (CFP 1100AE). The air flow rate was recorded when ramping up the air pressure to 250 kPa.

The tensile properties were tested on an Instron 5582 test frame according to ASTM D882-09. The strain ramp rate was 50%/minute.

The membrane wettability by a liquid electrolyte (1 M $LiPF_6$ in EC/DMC (1:1 by volume)) was performed by carefully applying a drop of the electrolyte on the membrane and observing its spread in 1 min.

The membrane thermal performance was evaluated using a dynamic mechanical analyzer (DMA Q800, TA Instruments) and a hot tip test. For the DMA tests, a preload force of 5 mN was applied and the temperature was ramped from 30 to 250 °C at a rate of 2 °C min^{-1}. Commercial polypropylene (PP) samples (Celgard 2400,

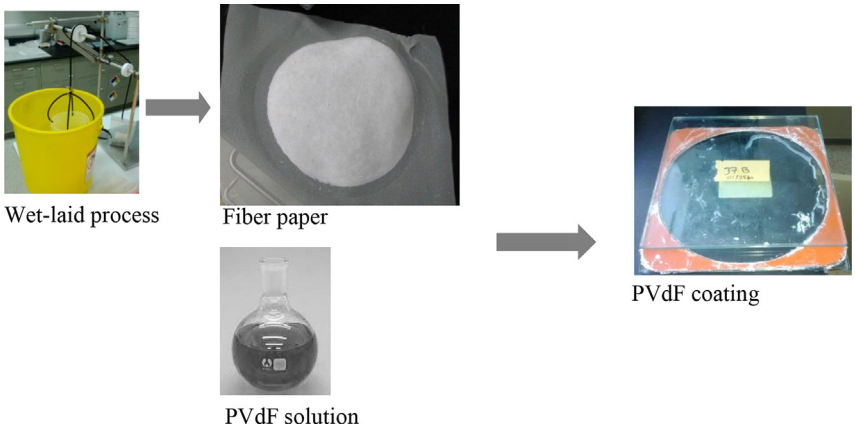

Fig. 1. Schematic of the preparation of the composite mats.

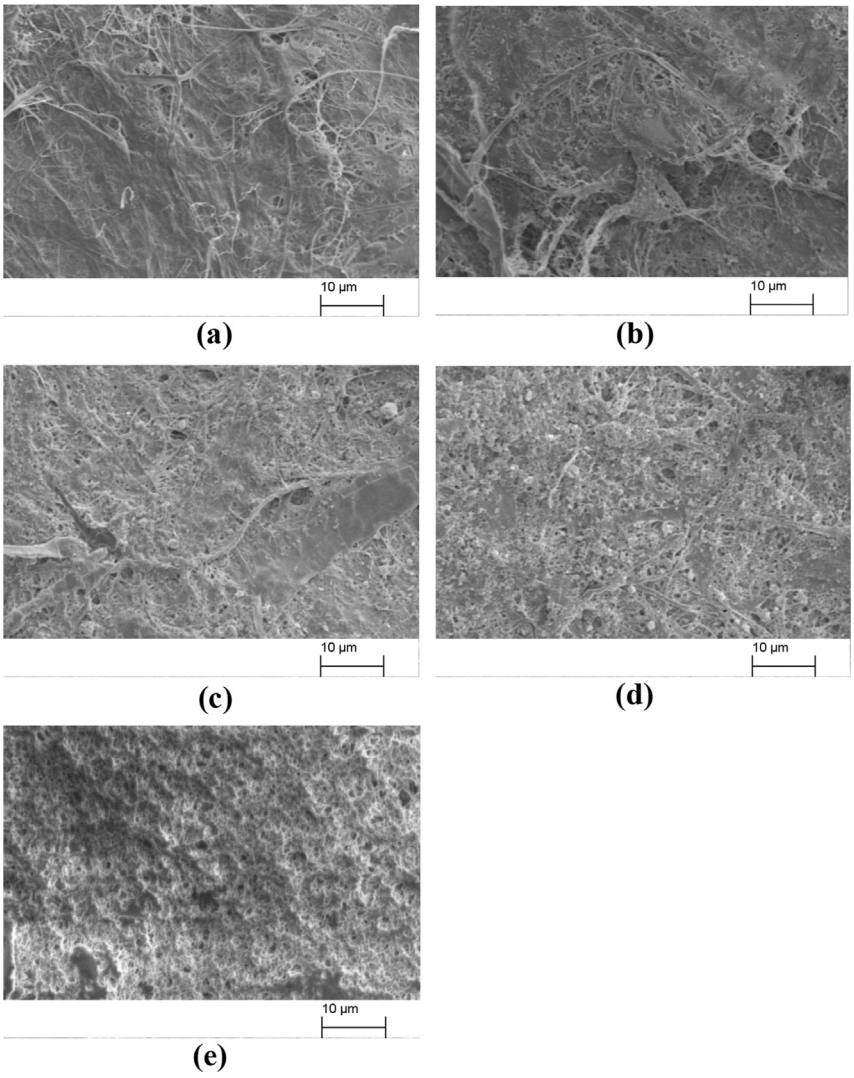

Fig. 2. SEM images of (a) MFC1, (b) MFC2, (c) MFC3, (d) MFC4, and (e) cMFC4.

25 μm thick) were tested in both machine direction (MD) and transverse direction (TD). In the hot tip tests, the diameter of the hole formed in the separator membrane in response to a hot wire in contact was measured. A 0.6 mm diameter copper wire heated to 300 °C was put in contact with the membrane sitting on an electrode and the diameter of the hole was recorded.

Ionic conductivity measurements were made on disc samples at 25 °C. The samples were saturated with a liquid electrolyte (1 M $LiPF_6$ in EC/DMC (1:1 by volume)) and sandwiched between two stainless steel electrodes. The bulk resistances were measured on an impedance gain analyzer (Solitron SI 1260, Princeton Applied Research) and the effective ionic conductivity values were calculated. Li/separator/Li symmetric cells were also assembled in a similar way and stored at 60 °C up to 5 days for the evaluation of the separator compatibility with metal lithium. The full cells with graphite anodes and NCM cathodes were assembled to evaluate the separator electrochemical performance. The cells were charged up to 4.3 V under a constant current–constant voltage mode, and then discharged under a constant current mode to 3.0 V on an Arbin Instruments cycler at room temperature. For the cycle tests, cells were charged and discharged at C/10 in the first 5 cycles and at C/5 in the following cycles. For the rate capability tests, cells were charged at C/10 and discharged at C/5, C/2, 1C, 2C, and 4C.

3. Results and discussion

Fig. 2 shows the images of different composite mats captured from SEM. The mats having MFC/alumina weight ratios of 1/0, 1/0.5, 1/1, and 1/1.5 are designated as MFC1, MFC2, MFC3, and MFC4,

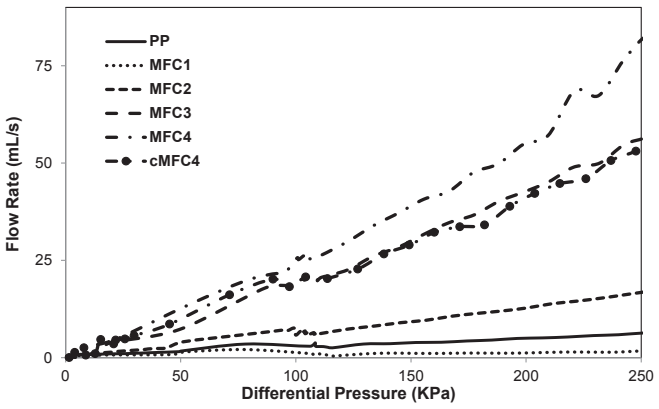

Fig. 3. Air permeability profiles of uncoated and coated separators.

Table 1
Effective ionic conductivity and tensile properties of the coated and un-coated separators.

Separator designation	Formulation (by weight)	Tensile strength (MPa)	Modulus (MPa)	Thickness (μm)	Effective conductivity (mS cm^{-1})	Porosity (%)
MFC1	MFC/alumina = 1/0	30.1 ± 0.8	1282 ± 125	23	0.14	16
MFC2	MFC/alumina = 1/0.5	20.7 ± 1.3	919 ± 69	24	0.52	36
MFC3	MFC/alumina = 1/1	12.2 ± 0.6	751 ± 88	25	1.06	54
MFC4	MFC/alumina = 1/1.5	8.6 ± 0.4	658 ± 87	28	1.28	68
cMFC4	PVDF coated MFC4	10.2 ± 0.8	506 ± 54	28	1.20	56

respectively. The PVDF coated MFC4 is designated as cMFC4. Fig. 2(a) is the image of MFC1. It can be seen that the cellulose fibrils are intermingled and randomly dispersed along the in-plane direction. The fibrils have a very wide diameter distribution ranging from a few nanometers to a few microns. The wide size distribution resulted in a very compact structure as the small fibrils filled in the pores formed by the big fibrils. Fig. 2(b)–(d) are the SEM images of MFC2, MFC3, and MFC4, respectively. Ceramic particles can be observed and the existence of the ceramic particles separated the fibrils resulting in open porous structures. The branching structure allowed the fibrils to entangle with each other, providing the necessary mechanical integrity. The porous PVDF coated MFC4 (cMFC4) is shown in Fig. 2(e). It is well known that PVDF/acetone/water systems can result in a porous structure with the evaporation of the solvent acetone due to the phase inversion process [14,15]. The porous PVDF phase ensured that the composite separator retained an open porous structure to allow a good ionic conductance, while keeping the ceramic particles from falling off when handling the composite membrane.

Fig. 3 shows the air flow rates through the membranes at different pressures. MFC1 had the lowest air permeability indicating a very compact structure, which is consistent with the SEM observation in Fig. 2(a). With the increase of the ceramic content, the mats showed increased air permeability. MFC2, MFC3, and MFC4 all exhibited higher air flow rates than the commercial separator. The coating by porous PVDF reduced the air flow rate even though the PVDF phase has a porous structure. The air permeability of cMFC4 was close to that of MFC3.

Table 1 lists the tensile properties and the effective ionic conductivity values of the composite separators. With the increase of the alumina content, the tensile strength of the mats decreased from about 30.1 MPa for MFC1 to about 8.6 MPa for MFC4. The modulus was also reduced from about 1282 MPa for MFC1 to about 658 MPa for MFC4. The incorporation of PVDF resulted in an increased tensile strength due to its binding effect, but a slightly decreased modulus. The tensile strength and modulus of cMFC4 were about 10.2 MPa and 506 MPa, respectively.

The effective ionic conductivities of the composite mats were also shown in Table 1. When saturated with a liquid electrolyte, the effective ionic conductivity enabled by MFC1 was only about 0.14 mS cm^{-1}. However, the incorporation of ceramic particles created an open porous structure resulting in an increased ionic conductivity. The effective ionic conductivities were increased to 0.52 mS cm^{-1}, 1.06 mS cm^{-1}, and 1.28 mS cm^{-1} for MFC2, MFC3, and MFC4, respectively. The higher ionic conductivities of the composite separators can be accredited to their open porous structures and high porosities, which is supported by the air permeability results in Fig. 3 and the porosity values in Table 1. One interesting observation is that MFC2 showed higher air permeability but lower ionic conductivity than the commercial separator. The reason behind this is not clear, but it might be related to the membrane deformation caused by the pressure applied in the air permeability tests. cMFC4 showed a slightly reduced ionic conductivity of 1.2 mS cm^{-1} compared to 1.28 mS cm^{-1} for MFC4. The PVDF phase may have filled some of the pores in MFC4 resulting in this slightly decreased ionic conductivity. This observation is also in agreement with the air permeability test results. The ionic conductivity enabled by the commercial separator used in this work in the presence of the same electrolyte was 0.96 mS cm^{-1}. Therefore, the composite

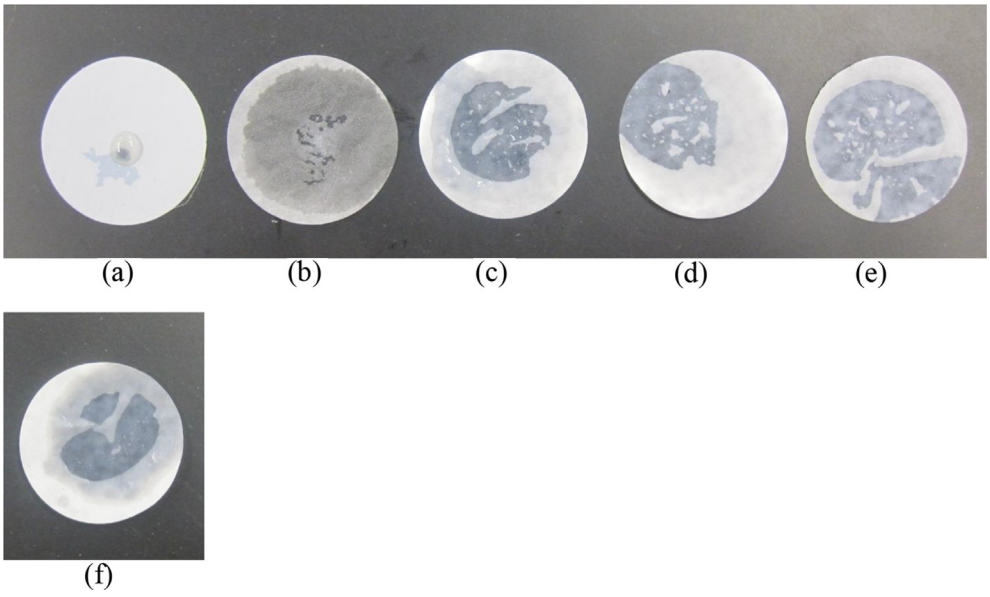

Fig. 4. Wettability test of uncoated and coated separators. (a) PP, (b) MFC1, (c) MFC2, (d) MFC3, (e) MFC4, and (f) cMFC4.

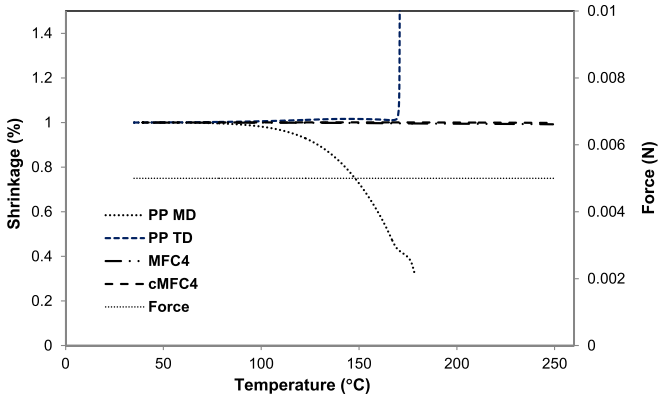

Fig. 5. Thermo-mechanical results (MFC separators vs. the commercial separator) from DMA. TD – transverse direction and MD – machine direction.

separators, especially MFC4 and cMFC4, showed higher effective ionic conductivity values.

The wettability of the separator by the electrolyte has shown to affect the overall electrolyte filling time of a battery [16,17]. The wettability test results were show in Fig. 4. These tests were conducted by simultaneously dropping a drop of electrolyte onto the surface of each separator and observing the spread of the electrolyte in 1 min. It is very clear that the electrolyte remained as a bead on the PP separator, although the visibly gray region indicates that the electrolyte has penetrated to the black bench top (used to provide contrast) through the separator. However, for the composite separators, the drops penetrated the mats and spread quickly in the mat in-plane direction. The rapid absorption and spreading of the electrolyte in the composite separators and on their surfaces is attributed to the high affinity of the liquid electrolyte to the cellulose fibrils, ceramic particles, and the PVDF binder.

Graphs of the composite mats and the commercial separator thermal response behaviors tested using DMA are displayed in Fig. 5. Both MFC4 and cMFC4 showed no evident shrinkages when the temperature was ramped up to 250 °C. The commercial separator shrank by 80% in the MD when the temperature was close to 180 °C. The melt of PP caused the abrupt increase in the elongation in the TD when the temperature was about 170 °C. The graphs of MFC1, MFC2, and MFC3 are not shown as they are very similar to those of MFC4 and cMFC4, and no evident shrinkages were observed.

Fig. 6 is the response of the separators to a simplified hot tip test. When the tip of the wire heated to 300 °C was in contact with the separator, the separator started melting at the contact point forming a hole around the wire tip. A small hole diameter may significantly reduce the consequences of an internal short in a battery because of the small contact area between the positive and negative electrodes. Fig. 6 indicated a melt hole of 1.7 mm in diameter in the PP separator, while the diameters of the holes formed in the composite separators were much smaller. It seems that the increase in the ceramic content reduced the diameter of the hole. For MFC4 and cMFC4, the damages due to the hot wire were much less severe compared to other tested membranes.

Fig. 7 shows the electrochemical impedance spectroscopy (EIS) of the symmetric Li cells with different separators, in which the large semicircle represents the impedance of the passivation layer formed on the surface of metal lithium, and the small semicircles are believed to be due to the impedances of charge-transfer and ionic diffusion through the interface. The cell with the commercial separator showed an initial low interfacial impedance, but it increased at a higher rate compared to the cells with the composite separators. After 5 days storage at 60 °C, the impedances of the passivation layers were much smaller in the case of MFC4 and cMFC4 cells compared to the PP separator.

The coin cell performance of the cells with the commercial separator, MFC2, MFC3, MFC4, and cMFC4 is shown in Fig. 8. The coin cell results of MFC1 separator were not included as the impedance of MFC1 is too high to make a coin cell with acceptable performance. It is observed that the cells with the composite separators showed stable performance on the repeated charging and discharging as shown in Fig. 8(a). This comparison demonstrates that the performance of the composite separators is quite encouraging. The slight difference on the specific capacities between different coin cells can be caused by the experimental deviations. The rate test results, in Fig. 8(b), indicate that the specific capacity retentions of the cells with different separators showed no significant difference to each other when the rate was below 1C. The cells with MFC4 and cMFC4 began to show better capacity retentions than the cell with the commercial separator in the subsequent

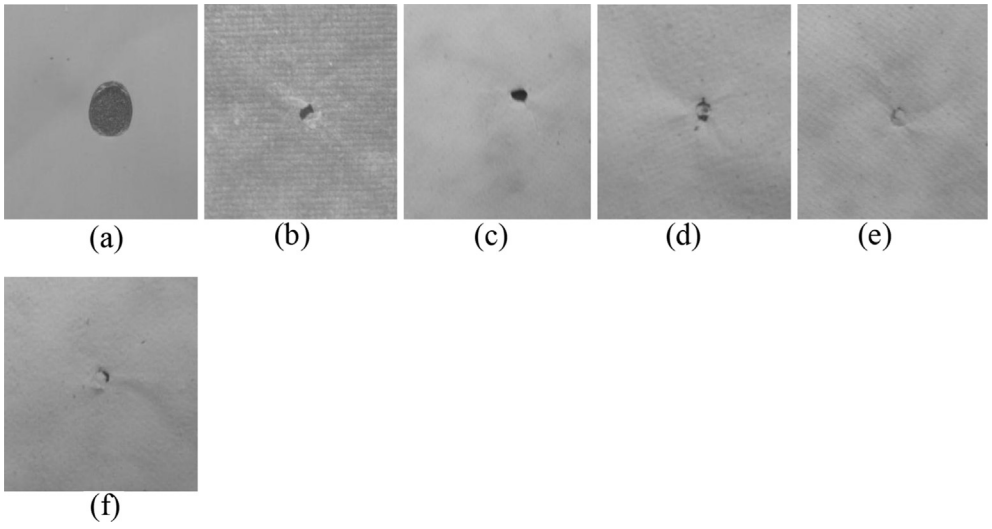

Fig. 6. Hot wire test of different separators at 300 °C. (a) PP, (b) MFC1, (c) MFC2, (d) MFC3, (e) MFC4, and (f) cMFC4.

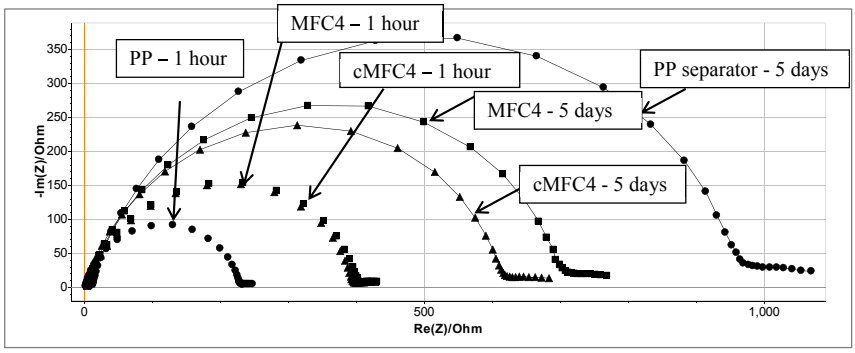

Fig. 7. Effect of storage time on the EIS of the symmetric lithium cells with different membranes.

discharge rates. This better rate performance is an indication of a low internal polarization, which can be contributed to the higher ionic conductivities enabled by the composite separators and their good wettability by the liquid electrolyte.

4. Conclusions

Composite separators, composed of micro-fibrillated cellulose (MFC), a ceramic powder, and an optional porous polyvinylidene fluoride (PVdF) binder/coating layer, were successfully developed using a low cost paper-making process. Dynamic mechanical analysis and a hot tip test were used to evaluate the thermal performance of the composite separators. The composite separators showed thermo-mechanical shrinkages of <1% when heated from 30 to 180 °C in air compared to the commercial counterpart shrinkage of 80% in the machine direction. The hot tip test results also supported the conclusion that the composite separators were more resistant to heat compared to the commercial separator as the diameter propagation of the formed hole in each composite separator in response to a hot spot was much smaller. Tensile testing of the PVdF coated and uncoated composite separators having a MFC/alumina weight ratio of 1/1.5 showed respective strength values of 10.2 MPa and 8.6 MPa, and respective Young's moduli of 506 MPa and 658 MPa. Their effective ionic conductivities, when saturated with an electrolyte of 1 M $LiPF_6$ in ethylene carbonate (EC)/dimethyl carbonate (DMC) (1:1 by volume), were 1.20–1.28 mS cm^{-1} (vs. 0.96 mS cm^{-1} enabled by the commercial separator). Electrochemical performance of the composite separators was studied in coin cells assembled using $LiNi_{1/3}Co_{1/3}Mn_{1/3}O_2$ cathodes, $LiPF_6$ in EC/DMC 1:1 (v/v) electrolyte, and graphite anodes. The cells with the composite separators showed stable cycle performance similar to that with the commercial separator. Cells with the composite separators, however, showed superior rate capabilities.

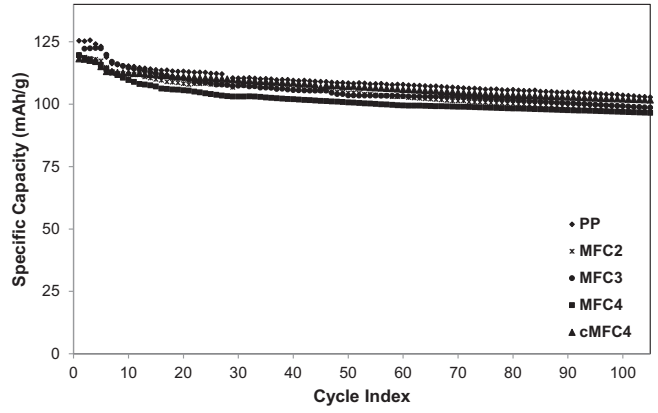

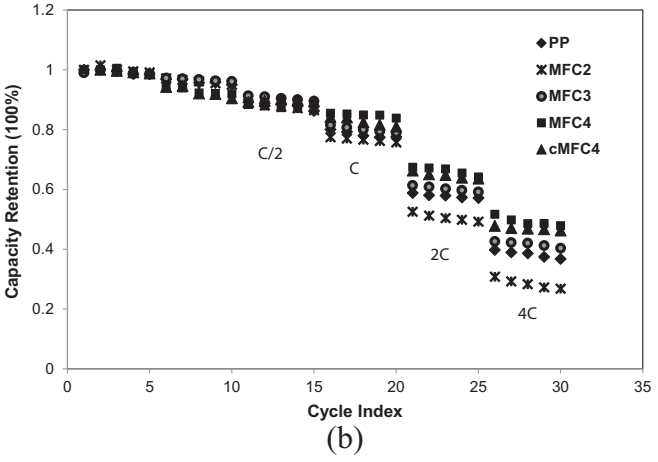

Fig. 8. Electrochemical performances. (a) Cycle tests and (b) rate tests for the cells with the composite and commercial separators.

Acknowledgments

The authors would like to recognize Li Yang, Jonathan Hitt, and Dongjoon Ahn for assisting with coin cell testing and their valuable discussions, and Yan Wu for her help in acquiring electrode materials.

References

[1] G.M. Ehrlich, in: D. Linden, T. Reddy (Eds.), Handbook of Batteries, third ed., McGraw Hill Books, New York, 2001, pp. 35.1–35.2.
[2] P. Arora, Z. Zhang, Chem. Rev. 104 (2004) 4419–4462.
[3] S.S. Zhang, J. Power Sources 164 (2007) 351–364.
[4] X. Huang, J. Solid State Electrochem. 15 (2011) 649–662.
[5] T.H. Cho, M. Tanaka, H. Onishi, Y. Kondo, T. Nakamura, H. Yamazaki, S. Tanase, T. Sakai, J. Power Sources 181 (2008) 155–160.
[6] S.W. Choi, S.M. Jo, W.S. Lee, Y.R. Kim, Adv. Mater. 15 (2003) 2027–2032.
[7] D. Bansal, B. Meyer, M. Salomon, J. Power Sources 178 (2008) 848–851.
[8] P. Kritzer, J. Power Sources 161 (2006) 1335–1340.
[9] T.H. Cho, M. Tanaka, H. Onishi, Y. Kondo, T. Nakamura, H. Yamazaki, S. Tanase, T. Sakai, J. Electrochem. Soc. 155 (2008) A699–A703.
[10] Y. Wang, H. Zhan, J. Hu, Y. Liang, S. Zeng, J. Power Sources 189 (2009) 616–619.
[11] S. Augustin, V. Hennige, G. Horpel, C. Hying, Desalination 146 (2002) 23–28.
[12] X. Huang, J. Hitt, J. Membr. Sci. 425 (2013) 163–168.
[13] X. Huang, A.N. Netravali, J. Macromol. Sci. A 45 (2008) 899–906.
[14] X. Huang, J. Power Sources 196 (2011) 8125–8128.
[15] X. Huang, J. Solid State Electrochem. 17 (2013) 591–597.
[16] Y.M. Lee, J.W. Kim, N.S. Choi, J.A. Lee, W.H. Seol, J.K. Park, J. Power Sources 139 (2005) 235–241.
[17] J. Saunier, F. Alloin, J.Y. Sanchez, G. Caillon, J. Power Sources 119–121 (2003) 454–459.